Chapter 18
Piezo Elements to Improve Dynamic Response of Load Cells

M. Vanali, C. Rossi, S. Pavoni, M. Berardengo, and S. Manzoni

Abstract This work addresses the passive reduction of structural vibration of a strain gauge load cell by means of shunted piezoelectric patches. The main goal of this work is the improvement of strain gauge load cells' dynamic behaviour increasing the damping coefficient. Tests have been firstly modelled and analyzed in ABAQUS commercial finite element (FE) code. Four piezoelectric patches were added in the regions of maximum deformation of the load cell to enhance their electromechanical coupling. Their performance is estimated in terms of the so-called electromechanical coupling factor (MEMCF), which is evaluated from forced-vibration analyses under short-circuit and open circuit electrodes of the patches. Piezo patches with similar geometrical and electrical characteristics and connections are so glued to the load cell. The addition of a negative capacitance in series to the resonant shunt shows an enhancement of its performance. The efficiency is evaluated in terms of MEMCF and attenuation of the resonant peaks. Experimental results have good agreement with the model, validating it.

Keywords Load cell · Piezoelectric shunt · Negative capacitance · Damping vibration control

Introduction

Strain gauge load cells are among the most widely employed force transducers in various applications, from industrial scales, for example in automatic weighing instruments, to automotive and aerospace engineering. They are appreciated for their accuracy, versatility and reliability. For example, they are employed in check weighers or weigh-price labellers. Since the performance of these machines is constantly improving, it is crucial to minimise the duration of the weighing process. The latter is linked to the load cell dynamic behaviour, both in terms of frequency response and time to settle after a perturbation is given. Therefore, the improvement of strain gauge load cells dynamic parameters, such as eigenfrequency and damping is a topic of great interest. The higher these parameters are the larger the bandwidth of the transducers will be, and the lesser the settling time will be. During the last years, researchers have focused on different aspects to enhance these performances. In some cases, the focus is on the post-processing of the signal, as in [1] where an adaptive filter is implemented to reduce the measurement time of a load cell, while others focus on the improvement of the bandwidth or the decrease of the settling time modifying the mechanical properties of the component. For example, M. Vanali et al. [2] employed AM techniques with damping materials to enhance the dynamic performance of a load cell by increasing its natural frequency.

In this work, the improvement of the transducer's mechanical properties, especially the damping ratio, is pursued through piezoelectric shunt damping associated with a specifically designed electrical network. This technique relies on the conversion of the mechanical energy to an electric energy that is dissipated through the resistive or a resonant component of a shunting electronic circuit [3]. Thomas et al. [4], [5] and Ducarne et al. [6] demonstrated that once the electric impedance is optimally tuned, the performance of the control depends only on the modal electromechanical coupling factor (MEMCF, k_i) of each mode of the electromechanical system (EMS) (approximating the system to a single degree of freedom system); the

M. Vanali · C. Rossi · S. Pavoni
Dipartimento di Ingegneria e Architettura, Università di Parma, Parco Area delle Scienze 181/A, 43124 Parma
e-mail: marcello.vanali@unipr.it; carlotta.rossi@unipr.it; stefano.pavoni@unipr.it

M. Berardengo
Dipartimento di Ingegneria Meccanica, Politecnico di Milano, Milano
e-mail: marta.berardengo@unige.it

S. Manzoni
Dipartimento di Ingegneria Meccanica, Energetica, Gestionale e dei Trasporti, Università degli Studi di Genova, Genova
e-mail: stefano.manzoni@polimi.it

Matthew Allen et al. (eds.), *Special Topics in Structural Dynamics & Experimental Techniques, Vol. 5*, Conference Proceedings of the Society for Experimental Mechanics Series, https://doi.org/10.13052/97887-438-0150-4_18

higher the MEMCF is, the higher the reachable attenuation and added damping is. This parameter can be easily evaluated since it is a function of the natural frequencies of the EMS in short circuit (SC) and open circuit (OC) of the mode considered through the formula:

$$k_i=\sqrt{\frac{\omega_{i\ OC}^2-\omega_{i\ SC}^2}{\omega_{i\ SC}^2}}\ where \tag{1}$$

$\omega_{\ iOC}$ is the ith natural frequency of the EMS in open circuit and $\omega_{\ iSC}$ is the ith natural frequency of the EMS in short circuit. Higher MEMCF can be obtained by choosing the best geometrical and electrical characteristics of the piezoelectric actuators, the best positioning of them, and adding a synthetic circuit, such as negative capacitances (NCs) to the shunt.

Starting from these bases the dynamic behaviour of the strain gauge cell was modelled and analyzed in ABAQUS commercial finite element (FE) code first.

Finite Element Model

As mentioned before, the strain gauge cell was first modelled using ABAQUS. The transducer understudy is a single-point load cell equivalent to the one produced by Laumas Elettronica S.r.l., FTP75 [7] model(75 kg full scale load). Our prototype is an additive manufacturing load cell produced with Atomic Diffusion Additive Manufacturing technique already studied by S. Pavoni et al. [2]. It is made with stainless steel 17-4 PH, a high resistance and hardness material with an ultimate tensile strength of 1250 MPa, yield strength of 1100 MPa and a tensile modulus of 170 GPa. The stressed areas of the load cell have been designed to maintain the component filled with material due to the thickness of the outer layers whereas the other parts follow a standard triangular 55% infill pattern with a 1 mm thickness. Its layout is reported in Figure 1.

It was found that the load cell's natural frequency increases by about 43% with the AM technique, while the critical damping ratio decreases. So, the dynamic parameters of the load cells are reported in Errore. L'origine riferimento non è stata trovata. below. For further details, refer to [2].

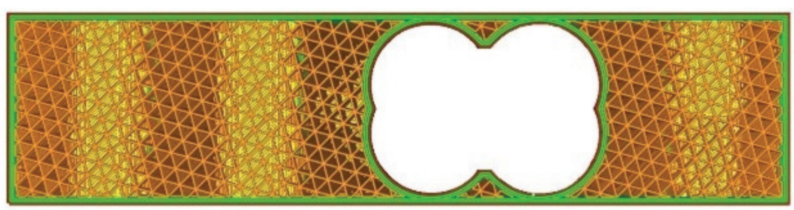

Fig. 1 Layout AM load cell.

Table 1 Dynamic characteristic of the AM load cell

Natural frequency [Hz]	Critical damping ratio (%)
817	0.1

The load cell has been modelled using linear brick elements (8-nodes, C3D8R where R is for reduced integration).

A preliminary FE free vibration analysis has been used to evaluate and compare the eigenfrequency of the first mode of the load cell to the experimental results obtained before [2], and so validate the FE model. The eigenfrequency of the first mode of the modelled load cell was found to be to 839.7 Hz, which can be considered to be in good agreement with the experimental one.

Moreover, the FE model has been used to identify the regions of maximum stress and strain in the cell. The piezoelectric patches have to be placed in these areas in order to maximize their electromechanical coupling and, consequently, the damping effect. Figure 2 shows clearly that regions with maximum stress and strain are in the four narrow areas where the central hole leaves a thin thickness with external edges, while Figure 3 shows the level of the strain (ε_{11}) in the upper central area.

Starting from these results, piezoelectric patches of different sizes have been added to the FE model in the regions with the maximum strain. The geometrical configurations have been chosen between those from the catalogue purchased by PI company for the bending piezoceramic sensor. All the patches are made in modified Lead Zirconate-Lead Titanate (identified by the company as PIC151) whose properties can be found on their website [8]

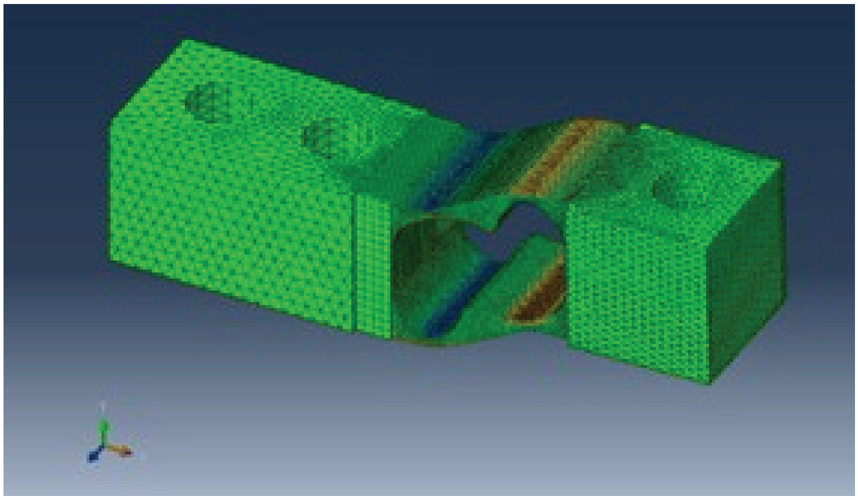

Fig. 2 FE model showing in red and blue the areas with maximum strain ε_{11}l.

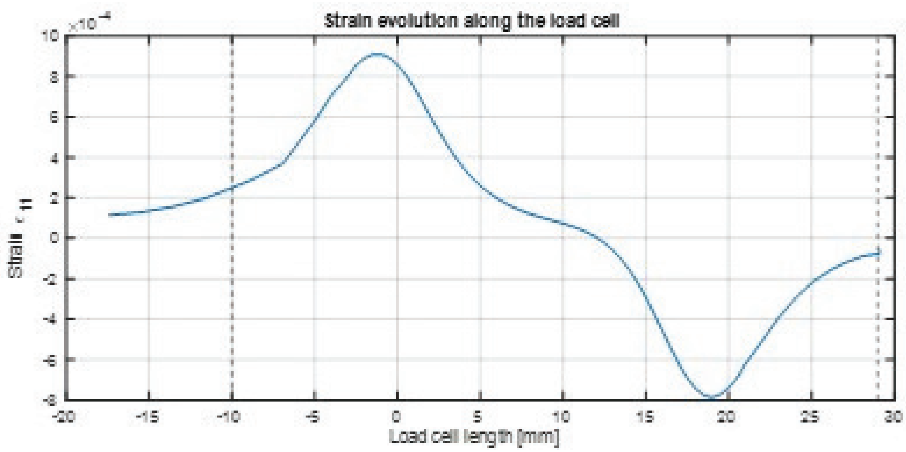

Fig. 3 Strain level along the central area of the load cell.

Every patch has been discretised using quadratic brick elements (20-nodes, C3D20RE where R is for reduced integration and E is for electric). Moreover, since the 4 main stressed areas show a symmetric deformation, two pairs of piezoceramic patches (PZT1-PZT3 and PZT2-PZT4) have been symmetrically bonded as shown in Figure 4

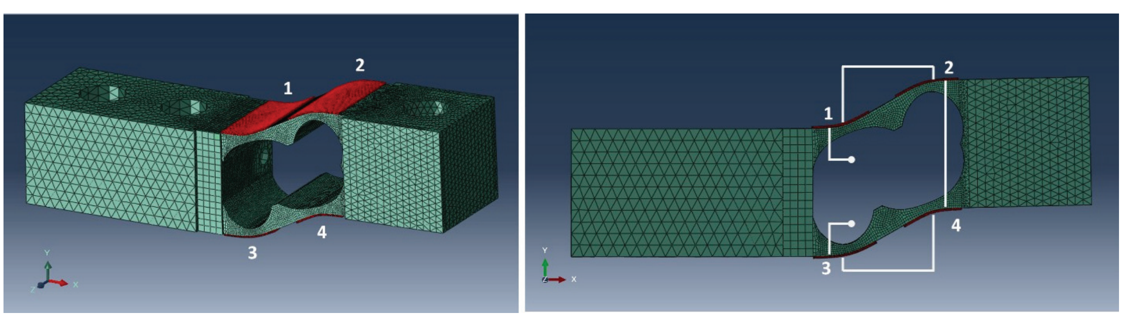

Fig. 4 FEM model with piezoelectric patches and their wiring connection.

The two pairs have the same poling direction, and so require electric parallel wiring. These connections produce opposite fields in the patches, so when the patch on the upper surface expands the one on the bottom surface contracts, creating a downward bending on the load cell. Then the two pairs are connected to each other with electric series wiring. The electric wiring connection between the patches has been created using the kinematic linear relation constraint on the electric degree of freedom (DOF9) of the external node surfaces of each patch. With these connections, to simulate the SC configuration it is required to apply zero potential to the surfaces of PZT1 and PZT3, while for the OC case one face has zero potential and the other one is charge-free. This solution has been chosen to maximize the attenuation given by the patches. Finally, the contact between the patches and the load cell is defined by Tie Constraint surface contact which ties two separate surfaces together so that there is no relative motion including rotation between them.

Free vibration analyses of the EMS have been performed in SC and OC of the mode being analyzed, to evaluate the MEMCF and thus the best piezoelectric patches geometrical characteristics.

Finite Element Results and Negative Capacitance Implementation

As discussed in the previous paragraph various geometrical layouts of the piezoelectric patches have been simulated. Some of them are reported in Table 2. In all the configurations the length of the patches is 28 mm, as the width of the load cell. The focus was to maximize the coupling factor trying to reduce the height of the patch as possible, in order to reduce its cost.

Table 2 Results obtained from different layouts of piezoelectric patches

Width x Height	Short Circuit Frequency	Open Circuit Frequency	Coupling Factor *k*
8 mm x 1 mm	957.89 Hz	969.04 Hz	0.15
8 mm x 0.75 mm	925.76 Hz	937.01 Hz	0.16
10 mm x 1 mm	989.65 Hz	1004.3 Hz	0.17
10 mm x 0.75 mm	946.34 Hz	960.34 Hz	0.17
12 mm x 1 mm	1032.4 Hz	1050 Hz	0.18
12 mm x 0.75 mm	983.37 Hz	999.15 Hz	0.18
12 mm x 0.5 mm	932.8 Hz	945.2 Hz	0.16
12 mm x 0.4 mm	912.77 Hz	923.25 Hz	0.15
12 mm x 0.25 mm	885.17 Hz	892.57 Hz	0.13
14 mm x 0.75 mm	999.58 Hz	1017.6 Hz	0.19
14 mm x 0.5 mm	941.1 Hz	954.69 Hz	0.17
14 mm x 0.4 mm	918.53 Hz	929.90 Hz	0.16
14 mm x 0.25 mm	886.6 Hz	894 Hz	0.13

The best solution was found to be the one with the patches of 28x14x0.75mm which ensure a MEMCF equal to 0.19. The most similar patch available in the PI catalogue with wrapped electrodes was 15x15x0.5 mm. The FE simulation of this patch resulted in ω_{SC} = 955.34 Hz, ω_{OC} = 955.34 Hz and *k* = 0.17.

Shunt Circuit

To enhance the performance of the shunt a synthetic circuit such as a negative capacitance (NC) can be added. Since in this case the attenuation has to be done on the first mode of the EMS the best NC layout is given by a series connection [9], [10] as shown in Figure 5.

In this case, an analogous term to the MEMCF, the enhanced modal electromechanical coupling factor (EMEMCF, $\tilde{k}_i$) is introduced, which accounts for the presence of the NC ($\tilde{k}_i > k_i$). This parameter, in a NC series connection, can be evaluated as follows:

$$\tilde{k}_i = \frac{k_i}{\sqrt{1 - \frac{C_{pi}}{C_2}}}, \; where \tag{2}$$

C_{pi} is the piezoelectric patch's capacitance at frequencies above ω_i and C_2 is the equivalent value of the NC.

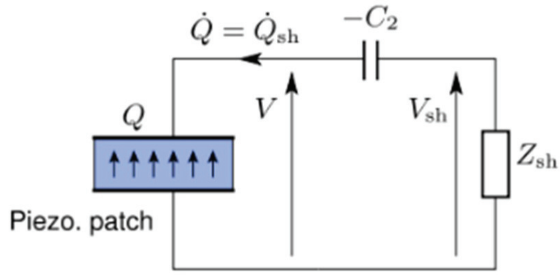

Fig. 5 Negative capacitance electrically connected in series to the piezo patch.

Negative Capacitance Optimisation

For the implementation and optimisation of the NC to be coupled to the circuit, the model developed by Thomas et al., Ducarne et al. and then improved by Berardengo et al. were used as reference [4], [9], [10]. First of all the capacitance of the piezoelectric patch Cpi, has to be evaluated.

The capacitance of the piezo patch was measured with a Hewlett-Packard 4284A LCR meter and resulted equal to 7.2 nF. To ensure the stability of the EMS the ideal value of C_2 must satisfy the condition: $C_2 > C_0$, where $C_0 = C_{pi} * (1 + k_i^2)$ for a series connection. The closer C_2 is to C_{pi}, thus to the stability limit, the higher EMEMCF is, and so the damping performance. To clarify further the effectiveness of the NC the index $\beta_2 = C_{pi} / C2$ is introduced [9]. The EMEMCF $\tilde{k}_i$enhanced by the NC in series so can be rewritten as:

$$\tilde{k}_i = \frac{k_i}{\sqrt{1 - \beta_2}} \tag{3}$$

Since the NCs do not exist in nature, they must be built synthetically, for example as in this work, through an OP-AMP. The circuit layout used in this case is shown in Figure 6.

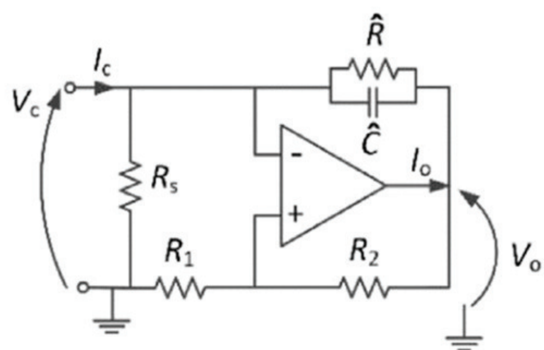

Fig. 6 Electrical layout of the NC implemented.

Notice that an additional resistance $\hat{R}$ is added to solve problems such as bias currents and also a compensation resistance R_s which improves the control performance and makes the circuit more robust to instability [9], [10].

The Optimisation results will be discussed in next section.

Experimental Tests

Starting from the results obtained from the FE simulations, the experimental tests have been carried out. The set-up consisted of the load cell mounted on a 1000 kg mass with two screws with a tightening torque of 40 Nm to avoid the influence of

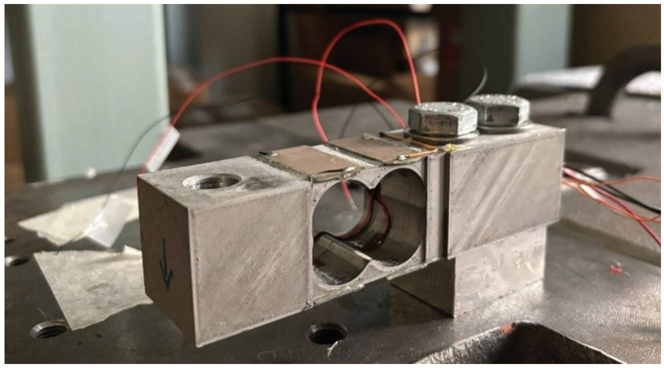

Fig. 7 Prototype of the load cell.

any external dynamics. Four piezoelectric patches with wrapped electrodes were bonded as shown in Figure 7 with an epoxy adhesive.

Unfortunately, the thin layer of adhesive used was not sufficient to electrically insulate the patches from the load cell. For this reason, the electrical circuit was modified as shown in Figure 8.

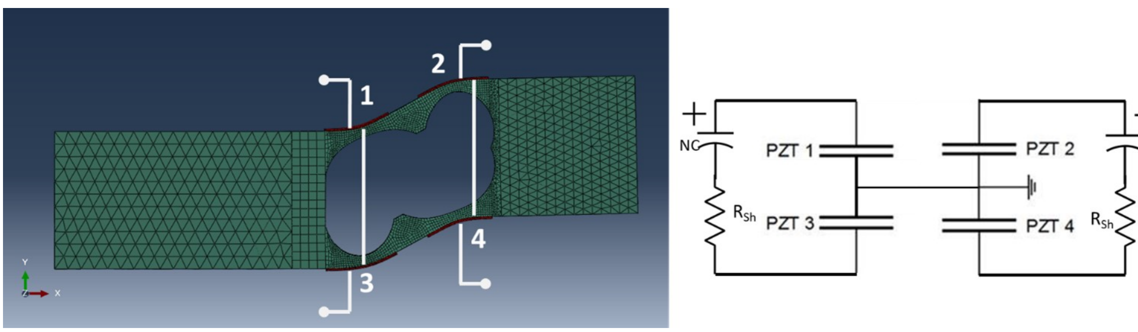

Fig. 8 New wiring connection and electrical layout.

The new layout consists of two pairs of piezoelectric patches (PZT1-PZT3 and PZT2-PZT4) with the same poling electrically connected in series. Then they are connected to the respective shunt circuit composed by the NC and the resistance R_{shunt}. Due to this, FE simulations with this new layout have been performed, to allow a correct construction of the NC.

The results of the two configurations are reported in Table 3 below:

Table 3 FEM results from the new piezoelectric layout

Parameter	PZT13 test	PZT24 test
$\omega_{SC}/(2\pi)$ [Hz]	957.02	958.71
$\omega_{OC}/(2\pi)$ [Hz]	964.38	964.38
k	0.124	0.109

In order to experimentally evaluate the dynamic parameters the load cell was excited with an impulsive method using an impact hammer. The FRF has been estimated with the H_1 estimator as

$$H_1 = \frac{G_{xy}(f)}{G_{xx}(f)}, \, where$$

$G_{xy}(f)$ is the cross spectrum between the load cell response and the hammer's one, and $G_{xx}(f)$ is the power spectrum of the hammer.

Being the system response basically a 1 DOF one, the eigenfrequencies and non-dimensional damping ratios have been evaluated using the peak picking method and the half power method. The k_i and $\tilde{k}_i$ values have been estimated by measuring the natural frequencies with the piezoelectric patches in SC, OC and with the working NC using the equation (1) and (2).

Finally, the optimal value for R_{shunt} to be connected in series to the NC was computed considering that:

$$R_{shunt}=\frac{\tau_e*(1-\beta_2)}{C_{pi}}\ ,\tau_e=\frac{1}{\omega_F}\text{with}\omega_F=\sqrt{\frac{\omega_{i\ OC}^2+\omega_{i\ SC}^2}{2}} \tag{4}$$

The NC has been built using Texas Instruments OPA445 OP-AMPs suiting the electrical scheme shown in Figure 6. The OP-AMPs were supplied with a direct current (DC) voltage of ± 45 V. The values of the different electric elements are reported in Table 4.

Table 4 Values of the parameters for the NC construction

Parameter	Value
R_1 [kΩ]	9.262
R_2 [Ω]	9.906
$\hat{R}$[MΩ]	0.800
$\tilde{R}$ [MΩ]	0.748
R_s [Ω]	0.756
$\hat{C}$ [nF]	7.480
C_2 [nF]	10.133
β_2	0.75

In the next section, the results of the experimental test will be discussed. Notice that, when one couple of piezoelectric patches was analysed, the other couple was in an OC condition. To be clearer, results will be presented as PZT13 for the couple PZTT1-PZT3 and PZT24 for the couple PZT2-PZT4, but the test procedure is the same.

Experimental Results

The natural frequencies of the load cell in SC and OC conditions are first estimated. After that, the NC is added in series to the circuit inducing a shift of the SC frequency to the left, and so, a higher coupling factor. Starting from these results the optimal value of R_{shunt} can be evaluated with 4. The same procedure was used during the test PZT24. The critical damping has been evaluated in the SC configuration and then with the R NC.

In Figure 9 the magnitude of the FRFs in the various electrical conditions for the two tests are reported. It is possible to notice that the shunt circuit implemented provides a good attenuation of the resonance peak to which it is tuned.

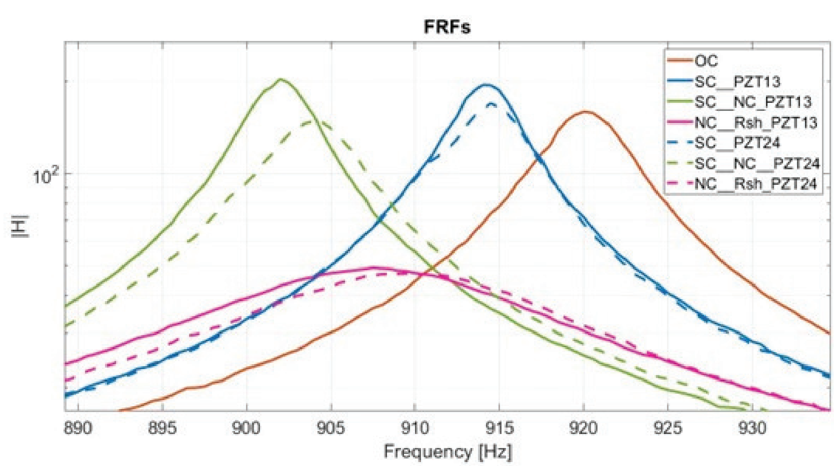

Fig. 9 RFs of the EMS obtained in different configurations (OC Open Circuit, SC Short circuit, NC Negative capacitance connected, NC-Rsh Negative capacitance with the resistive shunt connected).

Natural frequencies and damping ratios are reported in Table 5.

Table 5 Experimental results.

Parameter	Symbol	PZT13 test	PZT24 test
Natural Frequency in Short Circuit	$\omega_{SC}/(2\pi)$ [Hz]	914	915
Natural Frequency in Open Circuit	$\omega_{OC}/(2\pi)$ [Hz]	920	920
Modal electromechanical coupling factor	k	0.115	0.110
Natural Frequency in Short Circuit with NC connected	$\widehat{\omega_{SC}}/(2\pi)$ [Hz]	902	904
Natural Frequency in Short Circuit with NC and R_{shunt} connected	$\omega_{NCRSh}/(2\pi)$ [Hz]	909	910
Enhanced modal electromechanical coupling factor	$\tilde{k}$	0.201	0.189
Critical damping ratio in Short Circuit	ξ_{SC} (%)	0.27	0.29
Critical damping ratio with RNC connected	ξ_{RNC} (%)	1.29	1.12

All the tests have been re-done with the piezoelectric patches couple not investigated in SC instead of OC, but since they do not show significant variations compared to the results already obtained, they will not be reported. Moreover, comparing the results of the two tests it is noticeable that they are quite similar, confirming the symmetry of the EMS.

The addition of the Resistive Negative Capacitance shunt circuit results in the increment of the damping ratio ξ and of the natural frequency as shown in **Errore. L'origine riferimento non è stata trovata**.

Table 6 Natural frequencies and critical damping ratios comparison

	Natural frequency [Hz]	Critical damping ratio (%)
Additive Manufacturing	817	0.1
Additive Manufacturing and piezo in SC	914	0.27
Additive Manufacturing with shunt circuit	910	1.3

The improvement of the dynamic characteristic of the load cell can be established by both evaluating its bandwidth and settling time. In order to estimate the bandwidth, a single degree of freedom model was fitted with a least square method to experimental FRF. The bandwidth of transducers is computed starting from the magnitude value of the reconstructed FRF at 0 Hz, which represents the static sensitivity, with tolerance ranges equal to 1%, 5% and 10%. The reconstructed FRF is depicted in **Errore. L'origine riferimento non è stata trovata**.

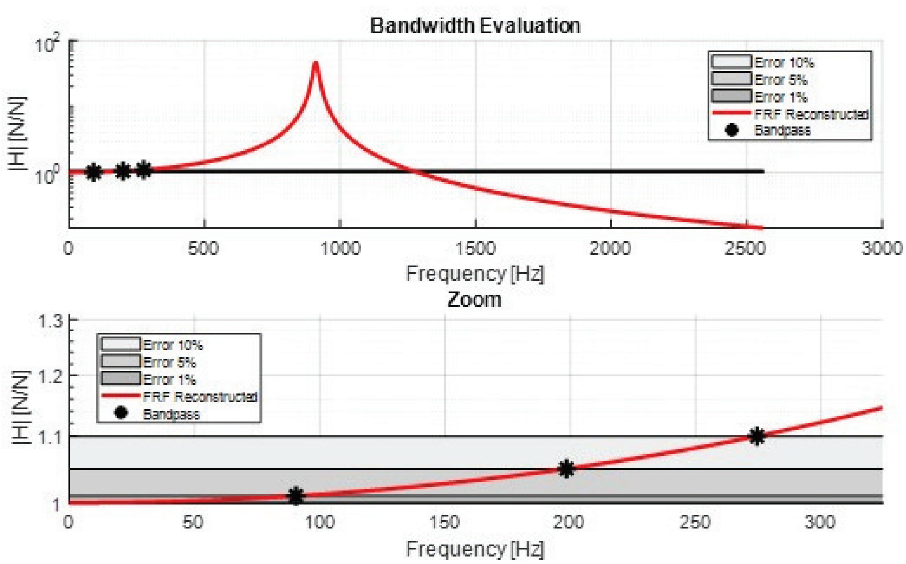

Fig. 10 Bandwidth evaluation for the load cell with shunt circuit connected.

Finally, the bandwidth was compared to the resulting one of the load cell without the shunt circuit, in order to evaluate the possible enhancement of the dynamic characteristics. Results are compared in Table 7.

Table 7 Bandwidth estimated from load cells

	High Cutoff Frequencies [Hz]		
Tolerance	1%	5%	10%
Additive Manufacturing	81	178	246
Additive Manufacturing with shunt circuit	91	199	275

Results show an increase in the bandwidth thanks to the shunt circuit of 10 Hz for 1% error, 21 Hz for 5% error and 31 Hz for 10% respectively. Thus, an average growth in bandwidth by about 12% is led by the shunt circuit.

Moreover the settling time of the load cell has been improved in the order of 1:10 as can be seen in the following graph (Figure 11).

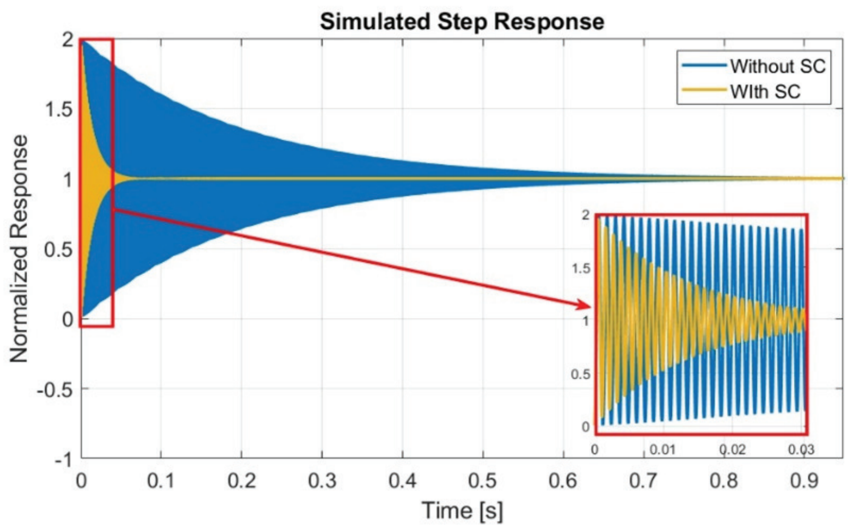

Fig. 11 Load cell settling time (Step response).

This improved settling time is meaningful in all those applications like filling machines where the step response is one of the driving parameters, and may lead to faster and more accurate measurements.

Conclusion

The aim of this work has been to enhance the dynamic characteristics of a single point load cell made by Additive Manufacturing through the implementation of piezoelectric shunts, precisely a resistive shunt coupled to negative capacitance. The FEM of the transducers was first developed in Abaqus software, to identify the areas with maximum stress and strain. Then, different piezoelectric patch layouts were simulated, with different sizes and electrical connections. The best configuration is the one which ensures the highest electromechanical coupling factor k. Starting from the numerical results, experimental tests have been carried out. To optimize the R NC layout the FRFs of the EMS in different electrical configurations have been implemented. Natural frequencies, MEMCFS, EMEMCFS and damping ratio have been evaluated. Experimental results are in good agreement with the numerical and theoretical ones. The damping ratio resulted in an enhancement from 0.27% to 1.3%. The resonance frequency increases too, from 817 Hz to 910 Hz. Finally, the load cell's bandwidth with the shunt circuit connected was evaluated. Bandwidth results prove an enhancement of dynamic characteristics, showing a 12% increment in bandwidth frequencies. Settling time was reduced in the order of 1:10, being this a real improvement in the cell performance.

Due to how the patches are bonded to the transducers, the two R NC shunts work separately and one at a time. So, in future works, the two R NC shunts working simultaneously will be tested. Finally, the patches will be rebounded to the transducers and the single electrical layout originally designed will be examined.

References

1. D. Richiedei, "Adaptive shaper-based filters for fast dynamic filtering of load cell measurements," *Mech Syst Signal Process*, vol. 167, p. 108541, Mar. 2022, doi:10.1016/j.ymssp.2021.108541.
2. M. Vanali, S. Pavoni, A. H. Lanthaler, and D. Vescovi, "Improving Dynamic Characteristics of Strain Gauge Load Cells Using Additive Manufacturing," 2024, pp. 163–172. doi: 10.1007/978-3-031-37007-6_18.
3. R. L. Forward, "Electronic damping of vibrations in optical structures," *Appl Opt*, vol. 18, no. 5, p. 690, Mar. 1979, doi:10.1364/AO.18.000690.
4. O. Thomas, J. Ducarne, and J.-F. Deü, "Performance of piezoelectric shunts for vibration reduction," *Smart Mater Struct*, vol. 21, no. 1, p. 015008, Jan. 2012, doi:10.1088/0964-1726/21/1/015008.
5. O. Thomas, J. -F. Deü, and J. Ducarne, "Vibrations of an elastic structure with shunted piezoelectric patches: efficient finite element formulation and electromechanical coupling coefficients," *Int J Numer Methods Eng*, vol. 80, no. 2, pp. 235–268, Oct. 2009, doi:10.1002/nme.2632.
6. J. Ducarne, O. Thomas, and J.-F. Deü, "Placement and dimension optimization of shunted piezoelectric patches for vibration reduction," *J Sound Vib*, vol. 331, no. 14, pp. 3286–3303, Jul. 2012, doi: 10.1016/j.jsv.2012.03.002.
7. "https://www.laumas.com/en/catalog/load-cells-and-mounting-kits-product-catalog-electronic-format-pdf/."
8. "www.PicaCeramic.com."
9. M. Berardengo, O. Thomas, C. Giraud-Audine, and S. Manzoni, "Improved resistive shunt by means of negative capacitance: new circuit, performances and multi-mode control," *Smart Mater Struct*, vol. 25, no. 7, p. 075033, Jul. 2016, doi:10.1088/0964-1726/25/7/075033.
10. M. Berardengo, S. Manzoni, O. Thomas, and M. Vanali, "Piezoelectric resonant shunt enhancement by negative capacitances: Optimisation, performance and resonance cancellation," *J Intell Mater Syst Struct*, vol. 29, no. 12, pp. 2581–2606, Jul. 2018, doi:10.1177/1045389X18770874.